

# A comparative study on dielectric behaviours of Au/(Zn-doped PVA)/*n*-4H-SiC (MPS) structures with different interlayer thicknesses using impedance spectroscopy methods

HAVVA ELİF LAPA<sup>1</sup>, ALI KÖKCE<sup>1</sup>, AHMET FARUK ÖZDEMİR<sup>1,\*</sup>, İBRAHİM USLU<sup>2</sup> and ŞEMSETTİN ALTINDAL<sup>3</sup>

<sup>1</sup>Department of Physics, Faculty of Sciences and Arts, Süleyman Demirel University, 32260 Isparta, Turkey

<sup>2</sup>Department of Chemistry Education, Faculty of Education, Gazi University, 06500 Ankara, Turkey

<sup>3</sup>Department of Physics, Faculty of Sciences, Gazi University, 06500 Ankara, Turkey

\*Author for correspondence (farukozdemir@sdu.edu.tr)

MS received 24 May 2017; accepted 7 November 2017; published online 23 May 2018

**Abstract.** Three different thicknesses (50, 150 and 500 nm) Zn-doped polyvinyl alcohol (PVA) was deposited on *n*-4H-SiC wafer as interlayer by electrospinning method and so, Au/(Zn-doped PVA)/*n*-4H-SiC metal–polymer–semiconductor structures were fabricated. The thickness effect of Zn-doped PVA on the dielectric constant ( $\epsilon'$ ), dielectric loss ( $\epsilon''$ ), loss-tangent ( $\tan \delta$ ), real and imaginary parts of electric modulus ( $M'$  and  $M''$ ) and ac electrical conductivity ( $\sigma_{ac}$ ) of them were analysed and compared using experimental capacitance ( $C$ ) and conductance ( $G/\omega$ ) data in the frequency range of 1–500 kHz at room temperature. According to these results, the values of  $\epsilon'$  and  $\epsilon''$  decrease with increasing frequency almost exponentially,  $\sigma_{ac}$  increases especially, at high frequencies. The  $M'$  and  $M''$  values were obtained from the  $\epsilon'$  and  $\epsilon''$  data and the  $M'$  and  $M''$  vs.  $f$  plots were drawn for these structures. While the values of  $\epsilon'$ ,  $\epsilon''$  and  $\tan \delta$  increase with increasing interlayer thickness, the values of  $M'$  and  $M''$  decrease with increasing interlayer thickness. The double logarithmic  $\sigma_{ac}$  vs.  $f$  plots for each structure have two distinct linear regimes with different slopes, which correspond to low and high frequencies, respectively, and it is prominent that there exist two different conduction mechanisms. Obtained results were found as a strong function of frequency and interlayer thickness.

**Keywords.** (Zn-doped PVA) interlayer; impedance spectroscopy method; frequency- and interlayer-thickness dependences; dielectric properties; electric modulus; ac conductivity.

## 1. Introduction

In recent years, many researchers have focused on the development or improvement in the metal–semiconductor (MS) structure by using high dielectric interfacial layer (i.e., BaTiO<sub>3</sub>, TiO<sub>2</sub>, GO-doped PrBaCoO nanoceramic, Bi<sub>2</sub>O<sub>3</sub>-doped PVA, graphene cobalt-doped Ca<sub>3</sub>Co<sub>4</sub>Ga<sub>0.0001</sub>O<sub>x</sub>, Bi<sub>3</sub>Ti<sub>4</sub>O<sub>12</sub> (BTO) and SrTiO<sub>3</sub> (STO)) [1–7]. The fundamental requirements for the materials are high dielectric constant, easy production and low-cost. Usually, for this aim, metal-doped polymers were examined as potential materials for replacing the conventional SiO<sub>2</sub> due to their some excellent features such as low-cost, simple fabrication and flexibility [3,8–12]. The high-dielectric interlayer can be used as an alternative to the conventional SiO<sub>2</sub> to decrease the serial resistance of the structure interface state ( $N_{ss}$ ) and increase of  $C$ . The use of high-dielectric interlayer can significantly increase the value of  $C$  and hence, can be more storage charges or energy [3,9]. In addition, the use of such high-dielectric interlayer can not only have the inter-diffusion between M and S but also acts a passivation effect. The quality, homogeneity, thickness and the dielectric constant value of interlayer

are also more important factors that affect the electrical and dielectric behaviours of these structures [13–15]. The presence of high dielectric interlayer prevents diffusion of charges at M/S interface and reduces the electric field relaxation in such structures.

There are various polymers such as polyaniline, polythiophene, P2ClAn and PVA [15–20]. Among them, PVA has attraction and attention due to its high dielectric strength, good charge storage capacity and excellent durability [14,21,22]. Generally, the electrical conductivities of pure polymers are poor, but their conductivity can be enhanced by doping with some metals (i.e., Co, Ni, Zn and Bi) [4,8–12]. Doping the polymers with suitable materials improves the charge-carrier transport ability in the host structure. On the other hand, doping the polymers may lead to a new application with the additional benefits offered by polymers in terms of mechanical properties [22].

The impedance spectroscopy method (capacitance–voltage ( $C$ – $V$ ) and conductance–voltage ( $G/\omega$ – $V$ )) measurements in wide range of frequencies and bias voltages can be supplied more and more information on the electric and dielectric characteristics of the metal/insulator or oxide/semiconductor

(MIS/MOS) and metal–polymer–semiconductor (MPS) type structures. In ideal case,  $C-V$  and  $G/\omega-V$  behaviours of these structures are independent of frequency [23]. This case, in practice, is very different particularly, at low frequency owing to the existence of  $N_{ss}$  localized at interlayer/semiconductor interface. Therefore, the investigations of the frequency-dependence dielectric parameters are very important especially, at wide range of frequencies. On the other hand, the oriental or dipole and interfacial polarization contribute to the  $\epsilon'$ ,  $\epsilon''$  and  $\sigma_{ac}$  values at low frequencies ( $f \leq 1$  MHz). Unlike low frequencies, the value of  $\epsilon'$  becomes closer to the value of  $\epsilon'$  at high frequencies and the  $N_{ss}$  cannot follow the alternating signal at high frequencies ( $f \geq 1$  MHz) [22,24,25].

To have a better understanding of the impact of frequency and interlayer thickness effect on  $\epsilon'$ ,  $\epsilon''$ ,  $\tan \delta$ ,  $M'$ ,  $M''$  and  $\sigma_{ac}$  of Au/*n*-4H-SiC structures with three different interlayer thicknesses (50, 150 and 500 nm) are fabricated and these parameters were investigated in the wide range of frequencies (1–500 kHz) at room temperature. Experimental results show that the use of Zn-doped PVA with 500 nm thickness leads to significant increase in the value of  $\epsilon'$  ( $> 2000$ ) and so can be more storage charges or energy compared to insulators such as SiO<sub>2</sub>, SnO<sub>2</sub>, Si<sub>3</sub>N<sub>4</sub> even at TiO<sub>2</sub>. In addition, all experimental results show that  $\epsilon'$ ,  $\epsilon''$ ,  $\tan \delta$ ,  $M'$ ,  $M''$  and  $\sigma_{ac}$  of Au/*n*-4H-SiC structures are considerably dependent on frequency and interfacial/interlayer thickness.

## 2. Experimental

In this work, the Au/(Zn-doped PVA)/*n*-4H-SiC (MPS) structures with three different interfacial layer thicknesses were prepared on *n*-type 4H-SiC wafers with a (100) orientation,  $7.07 \times 10^{17} \text{ cm}^{-3}$  doping concentration and 250  $\mu\text{m}$  thickness. To obtain a clean surface, before fabrication, chemical cleaning procedures were performed in the ultrasonic bath with 40 kHz frequency. After each cleaning step, wafers with 18 M $\Omega$  resistivity were rinsed in deionized (DI) water for about 10 min. In the first step, the *n*-4H-SiC wafers were ultrasonically cleaned in trichloroethylene and ethanol for  $\sim 5$  min and then rinsed in DI water for 10 min. In the second step, they were ultrasonically polished in aqua regia (CP4) for 30 s and then rinsed with propylene glycol. Then, these wafers were polished in H<sub>2</sub>SO<sub>4</sub>, H<sub>2</sub>O<sub>2</sub> and 20% HF solutions, and dried again in DI water. To prevent native oxidation, 4H-SiC wafers dried with dry nitrogen (N<sub>2</sub>) gas. After cleaning processes, wafers were inserted into the deposition chamber. Then, the high pure (99.999%) gold (Au) with thickness of 150 nm was thermally evaporated onto the back side of the *n*-4H-SiC wafers in high-vacuum metal evaporation system at  $1.33 \times 10^{-7}$  kPa. To perform good/low resistivity ohmic back contact, these structures were annealed at 500 °C for 5 min in flowing dry N<sub>2</sub> atmosphere.

To form MPS structures, the prepared PVA (Zn nanoparticle-doped) solution was grown on the front of 4H-SiC wafers

using the electrospinning method as interfacial layer. Thickness values of deposited PVA interfacial layers were measured with VeecoDektak 6 M thickness profilometer. Obtained values were recorded as 50, 150 and 500 nm, and the structures corresponding to these interfacial layer thickness values will be called as MPS-50 nm, MPS-150 nm and MPS-500 nm, respectively. After the deposition of PVA interfacial layers, the Schottky or rectifier contacts were formed thermally evaporating Au as dots (through a metal shadow mask) with determined dimension (a diameter of  $\sim 10$  nm and thickness of 150 nm) onto front surface of the PVA/*n*-4H-SiC/Au (structure area =  $3.14 \times 10^{-2} \text{ cm}^2$ ). Thus, the Au/(Zn-doped PVA)/*n*-4H-SiC (MPS) structures were prepared. Both the prepared (Zn-doped PVA) and the schematic diagram of the Au/(Zn-doped PVA)/*n*-4H-SiC (MPS) structure are shown in figure 1a and b, respectively. The surface images of the prepared Zn-doped PVA layer on the *n*-4H-SiC were taken by a JEOL JSM-6060LV scanning electron microscope (SEM). As shown in figure 1a, SEM observations give microscopic information about the surface structure of Zn-PVA material and revealing the nonwoven and interconnected structure of the nanofibres. Spinning of the Zn-PVA solutions resulted in uniform fibres with a broad distribution of the fibre diameter. Electrospun architecture seems as non-porous smooth polymer nanofibre. It is clear that the Zn-PVA film was successfully deposited on the *n*-4H-SiC surface by electrospinning method.

To perform the impedance measurements, the fabricated Au/*n*-4H-SiC (MPS) structures with three different interlayer thicknesses of Zn-doped PVA were mounted on a copper holder with the help of silver dag and the electrical contacts were made to the upper electrodes by the use of tiny silver-coated wires with silver paste. Thus, at room temperature, to perform capacitance–voltage–frequency ( $C-V-f$ ) and conductance–voltage–frequency ( $G/\omega-V-f$ ), measurements of prepared structures have used HP4192A LF impedance analyzer (5 Hz–13 MHz) and a microcomputer through an IEEE-488 AC/DC converter card. All the measurements were performed in the frequency range of 1–500 kHz and the dc bias voltage was swept from  $-6$  V to  $+6$  V by 50 mV steps.

## 3. Results and discussion

The  $\epsilon'$ ,  $\epsilon''$ ,  $\tan \delta$ ,  $\sigma_{ac}$ ,  $M'$  and  $M''$  parameters were calculated using  $C$  and  $G$  data for Au/(Zn-doped PVA)/*n*-4H-SiC (MPS) structures by using the following expressions [7,22,26–31]:

$$\epsilon' = \frac{C}{C_0} = \frac{Cd}{\epsilon_0 A}, \quad (1a)$$

$$\epsilon'' = \frac{G}{\omega C_0} = \frac{Gd}{\epsilon_0 \omega A}, \quad (1b)$$

$$\tan \delta = \frac{\epsilon''}{\epsilon'}, \quad (1c)$$

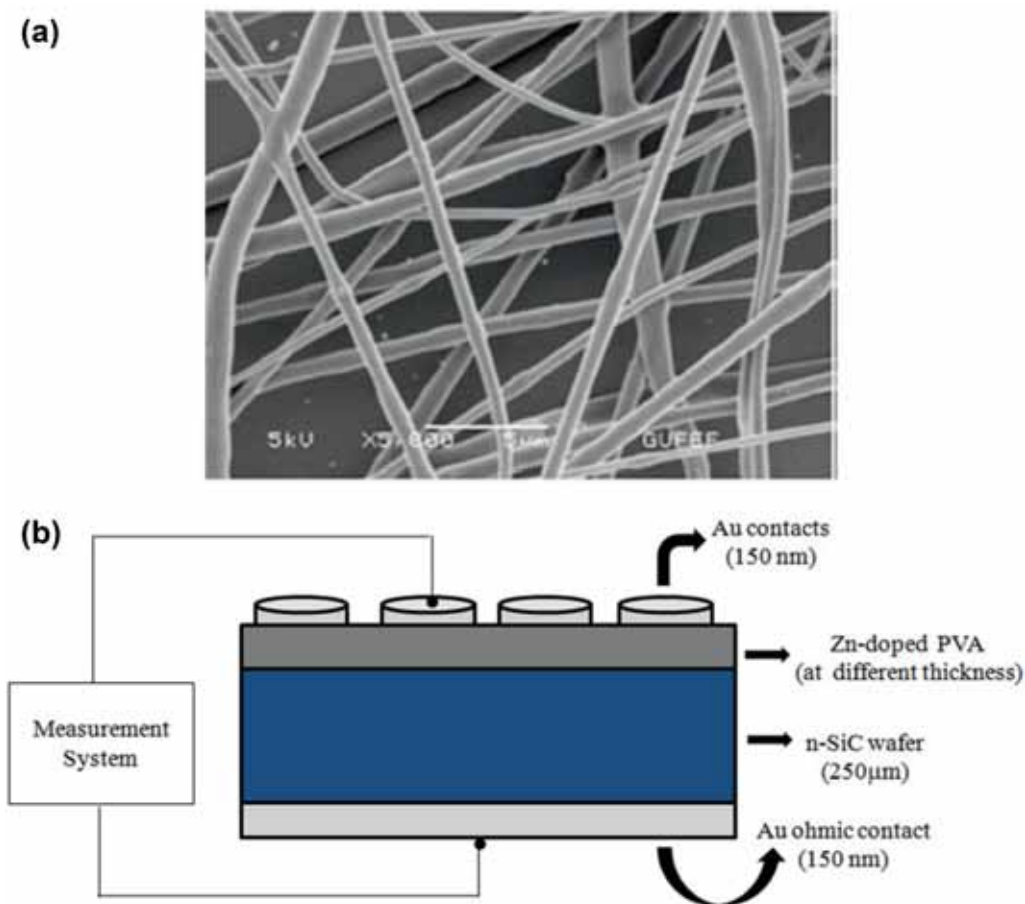


**Figure 1.** (a) SEM image of Zn-doped PVA polymeric interfacial layer and (b) schematic diagram of the Au/(Zn-doped PVA)/n-4H-SiC (MPS) structure.

$$\sigma_{ac} = \omega C \tan \delta (d/A) = \varepsilon'' \omega \varepsilon_0, \quad (2)$$

$$M^* = \frac{1}{\varepsilon^*} = M' + jM'' = \frac{\varepsilon'}{\varepsilon'^2 + \varepsilon''^2} + j \frac{\varepsilon''}{\varepsilon'^2 + \varepsilon''^2}. \quad (3)$$

Here,  $\varepsilon_0$ ,  $\omega$ ,  $A$ ,  $d$  are respectively, the permittivity of free space ( $= 8.85 \times 10^{-14} \text{ F cm}^{-1}$ ), the angular frequency ( $= 2\pi f$ ), the rectifier or Schottky contact area and the interfacial layer thickness [3,26]. The frequency dependence of some dielectric parameters (i.e.,  $\varepsilon'$ ,  $\varepsilon''$  and  $\tan \delta$ ) for 6 V were obtained using equation (1a–c) for Au/n-4H-SiC (MPS) structures with three different (50, 150 and 500 nm) thickness interfacial (Zn-doped PVA) layers. Figure 2a–c exhibit the values of these parameters as function of frequency measured in the range from 1 to 500 kHz with an ac oscillation voltage ( $V_{oc}$ ) of 40 mV. In figure 2, the values of these parameters for each structure decrease with increasing frequency almost as exponentially. On the other hand, these values increase with increasing interfacial layer thickness, but these values become almost independent of thickness at high frequencies. The value of  $\varepsilon'$  for MPS with 500 nm interlayer thickness was found at about 2120 even at 1 kHz, which is 558 times greater

than the dielectric value of  $\text{SiO}_2$  and 42 times greater than the dielectric value of  $\text{TiO}_2$ . These results show that the use of Zn-doped PVA interlayer with enough thickness (500 nm), not only increases the capacitance, but also increases charges or energy storage compared to the traditional insulator/oxide (i.e.,  $\text{SiO}_2$  or  $\text{SnO}_2$ ). Namely, to get an ultra-high capacitor, the high dielectric interlayer can be used. Hence, to increase the capacitance, one has to increase  $\varepsilon'$  and decrease the thickness of interlayer; however, value of the thickness of interlayer is largely determined by the working voltage and cannot be tampered [32].

When the thickness of interlayer is higher than a few hundreds, metal/semiconductor structures act as a MIS or MPS type capacitors rather than diode. Capacitors are fundamental electric circuit elements that store electric charges or electrical energy. To increase the capacitance ( $C = \varepsilon' \varepsilon_0 A/d = \varepsilon' C_0$ ), the decrease of  $d$  and the increase of  $\varepsilon'$  or  $A$  are required. Here,  $C_0$  is the value of the empty capacitor. On the other hand, the magnitude of dielectric constant especially at low frequencies is dependent on the existence of surface states and space-charge polarization [25]. Therefore, high values of  $\varepsilon'$  and  $\varepsilon''$  for high  $d$  is the result of the low value of  $C_0$ . The interfacial insulator/polymer materials can be easily polarized

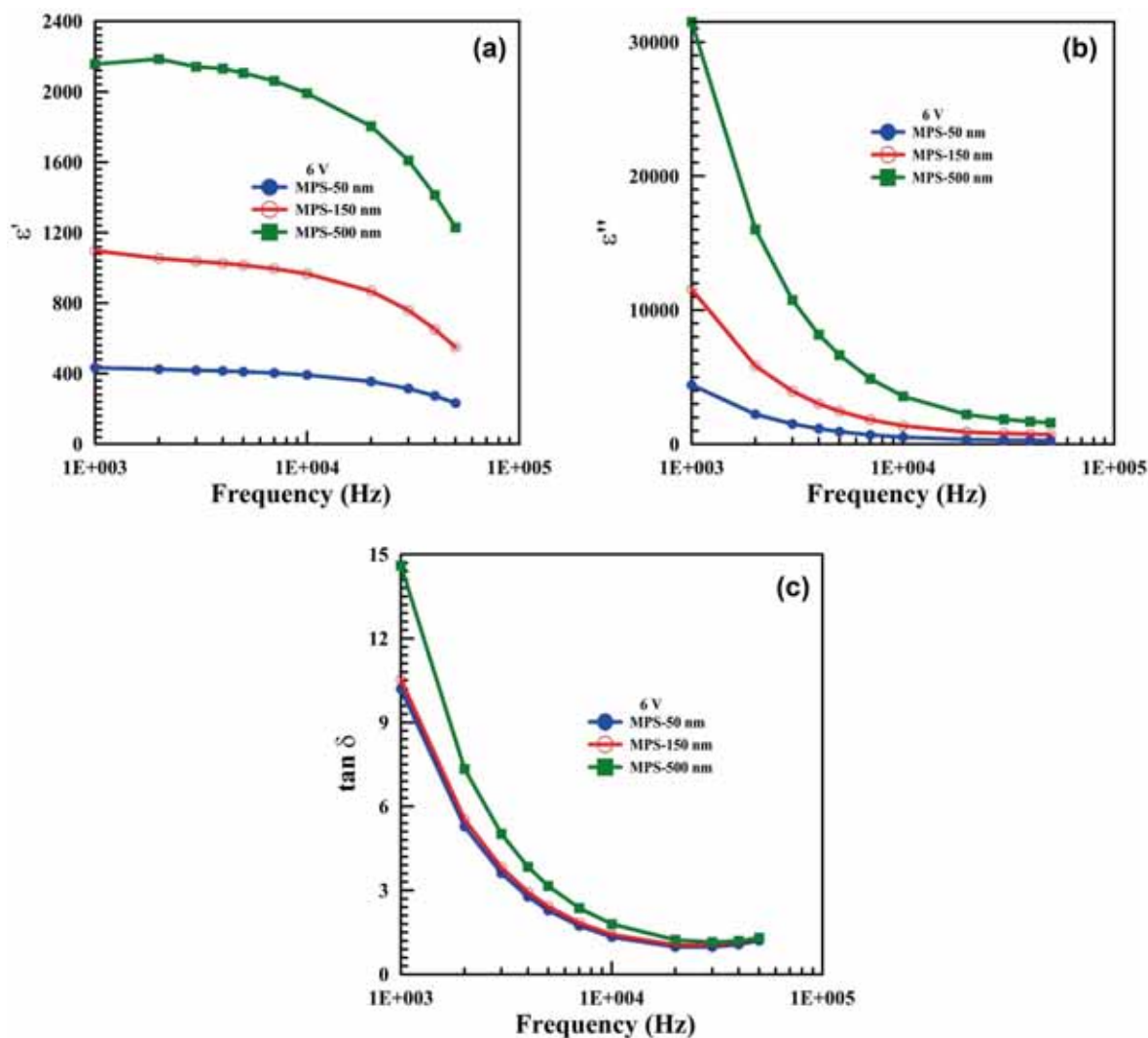


**Figure 2.** (a–c) Frequency dependence of  $\epsilon'$ ,  $\epsilon''$  and  $\tan \delta$  for Au/*n*-4H-SiC (MPS) structures with three different thickness (50, 150, 500 nm) interfacial (Zn-doped PVA) layers at room temperature.

under an external electric field that displaces the charges from their equilibrium position or traps. Namely, the charges or dipoles can be restructured and reordering under electric field depends on their relaxation times. There are many kinds of surface states or traps with different lifetimes and at low frequencies, these states affected by the applied signal, are able to give up and accept charges in response to this signal. Recently, research study on the modification of the conventional MOS capacitors to increase the specific capacitance is also in progress [32]. In addition, in figure 2a–c, the values of  $\epsilon'$ ,  $\epsilon''$  and  $\tan \delta$  are dependent on frequency and interfacial layer thickness and these values decrease not only with increasing frequency, but also with increasing interfacial layer thickness between M and S. Here, the thickness of interfacial layer and its homogeneity are more effective on the impedance measurements. However, the values of these parameters are also dependent on the applied bias voltage, but the real values

are corresponding to the strong accumulation region of  $C-V$  and  $G/\omega-V$  characteristics [25,26]. The strong accumulation region is corresponding to the 6 V for our structures.

The  $M'$  and  $M''$  values were obtained from equation (3) and are presented in figure 3a and b, respectively. In figure 3, both the values of  $M'$  and  $M''$  increase with increasing frequency, whereas decrease with increasing the thickness of interfacial layer. The value of  $M'$  reaches a maximum value for three different thicknesses of interfacial layer at high frequency, which are corresponding to the  $M_\infty = 1/\epsilon_\infty$  owing to relaxation process. Additionally, the values of  $M'$  approach almost zero, confirming that the elimination of electronic polarization took place [25,26,33]. Such behaviour of  $M'$  with frequency can be ascribed to the conduction phenomena because of the short range mobility of charge carriers localized at interfacial layer/s in the forbidden band gap. The changes in  $\epsilon'$ ,  $\epsilon''$  and  $\tan \delta$  values are the result of a special distribution of surface



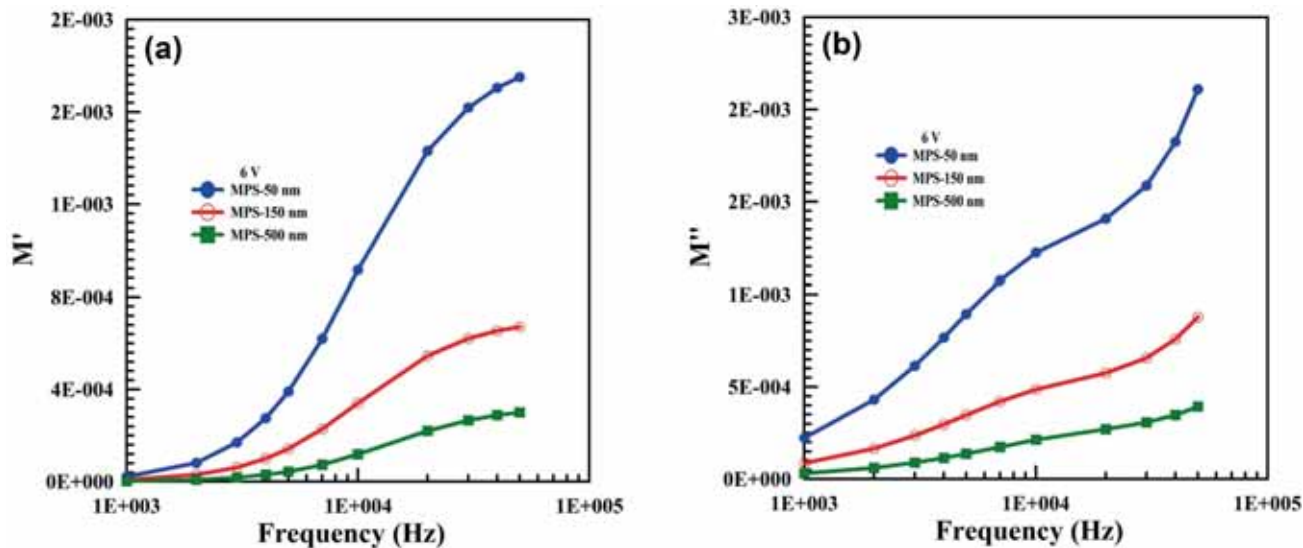


**Figure 3.** Frequency dependence of  $M'$ ,  $M''$  vs.  $f$  plots of the Au/ $n$ -4H-SiC (MPS) structures with three different thickness (50, 150, 500 nm) interfacial (Zn-doped PVA) layers at room temperature.

states and their relation time, surface-dipole polarization, used interlayer thickness at M/S interface and its homogeneities.

The values of  $\sigma_{ac}$  for Au/(Zn-doped PVA)/ $n$ -4H-SiC (MPS) structures were calculated from equation (2) and the double logarithmic  $\sigma_{ac}$  vs.  $f$  plots were given in figure 4. As shown in figure 4, these plots have two distinct linear regions with different slopes, which are corresponding to low and high frequencies. This situation is an evidence to the existence of two different conduction mechanisms in these structures. The electric response of the low conductivity materials is usually given as follows [34–36]:

$$\sigma(\omega) = \sigma(0) + A\omega^s, \tag{4}$$

where  $\sigma(0)$  is the frequency-independent dc (or low-frequency) conductivity,  $A$  and  $s$  are fitting parameters. The frequency-dependent conductivity can also be obtained from the following equation [35]:

$$\sigma(\omega) = \sigma(0) + A_1\omega^{s_1} + A_2\omega^{s_2}. \tag{5}$$

Here, the first ac term dominates at low frequencies (we denote the region as i), corresponding to translational hopping motion ( $0 < s_1 < 1$ ). The second ac term dominates at high frequencies (we denote the region as ii), and corresponds to well-localized hopping and/or reorientational motion ( $1 < s_2 < 2$ ). The values of  $s_1$  were determined from the slope of  $\ln(\sigma_{ac})$  vs.  $\ln f$  linear region as 0.059, 0.051 and 0.039 at region i and 0.613, 0.597 and 0.499 at region ii, for MPS-50 nm, MPS-150 nm and MPS-500 nm, respectively. These values show the existence of hopping mechanisms ( $0 < s_1 < 1$ ).

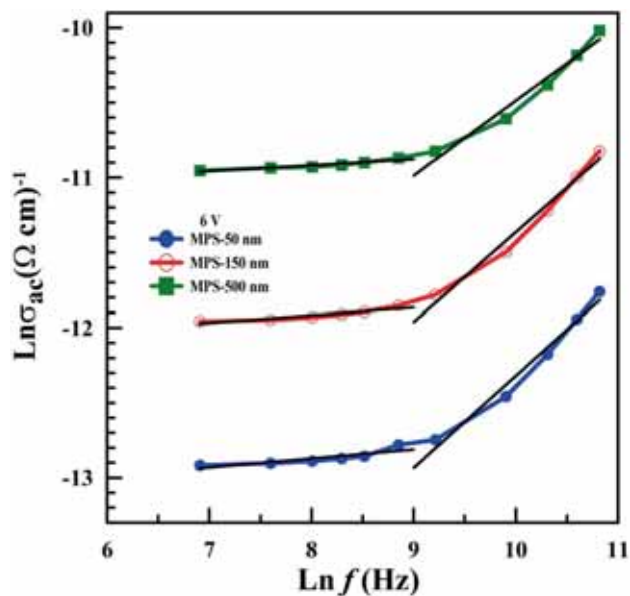


**Figure 4.** Frequency dependence of  $\ln \sigma_{ac}$  vs.  $f$  plots of the Au/ $n$ -SiC (MPS) structures with three different thickness (50, 150, 500 nm) interfacial (Zn-doped PVA) layer at room temperature.

#### 4. Conclusions

The Au/ $n$ -4H-SiC (MPS) structures with three different thicknesses (50, 150 and 500 nm) interfacial (Zn-doped PVA) layers were fabricated. Both the frequency (1–500 kHz) and interlayer thickness dependences of  $\epsilon'$ ,  $\epsilon''$ ,  $M'$ ,  $M''$  and  $\sigma_{ac}$  of these fabricated samples were investigated in detail by using impedance spectroscopy method and compared at room temperature. Obtained parameters depend on frequency and interfacial layer thickness, particularly at low frequencies and

accumulation region. The values of  $\varepsilon'$ ,  $\varepsilon''$  and  $\tan \delta$  decrease not only with increasing frequency, but also with increasing interfacial layer thickness between M and S. The values of  $M'$ ,  $M''$  and  $\sigma_{ac}$  increase with increasing frequency. In addition, the dispersion in the dielectric properties can attribute to particular density distribution of the  $N_{ss}$ -localized PVA/*n*-4H-SiC interface as well as space-charge carriers and thickness of the interfacial polymer layer. The  $\sigma_{ac}$  vs.  $f$  plot for each structure has two distinct linear regions with different slopes, which are corresponding to low and high frequencies. This situation can be explained by the existence of two different conduction mechanisms in these structures. In conclusion, all these results indicated that the dipole and interfacial polarizations can be occurred at low and intermediate frequencies and additional carrier charges at surface states or interface traps can easily follow the applied ac signal and yield an excess of  $C$  and  $G$ .

### Acknowledgements

This study was supported by The Management Unit of Scientific Research Projects of Süleyman Demirel University (SDUBAP) under 4611-D2-16. We wish to thank SDUBAP for contributions.

### References

- [1] Reddy V R, Manjunath V, Janardhanam V, Kil Y H and Choi C J 2014 *J. Electron. Mater.* **43** 3499
- [2] Asar Şafak Y, Asar T, Altındal Ş and Özçelik S 2015 *J. Alloys Compd.* **628** 442
- [3] Kaya A, Alialy S, Demirezen S, Balbaş M, Yerişkin S A and Aytimur A 2016 *Ceram. Int.* **42** 3322
- [4] Gökçen M, Tunç T, Altındal Ş and Uslu İ 2012 *Curr. Appl. Phys.* **12** 525
- [5] Kaya A, Maril E, Altındal Ş and Uslu İ 2016 *Microelectron. Eng.* **149** 166
- [6] Durmuş P, Yıldırım M and Altındal Ş 2013 *Curr. Appl. Phys.* **13** 1630
- [7] Liu C Y and Tseng T Y 2004 *Ceram. Int.* **30** 1101
- [8] Tunç T, Altındal Ş, Dökme İ and Uslu H 2011 *J. Electron. Mater.* **40** 157
- [9] Yerişkin S A, Balbaş M and Tataroğlu A 2016 *J. Appl. Polym. Sci.* <https://doi.org/10.1002/APP.43827>
- [10] Kaya A, Yücedağ İ, Tecimer H and Altındal Ş 2014 *Mater. Sci. Semicond. Process.* **28** 26
- [11] Çicek O, Uslu Tecimer H, Tan S O, Tecimer H, Altındal Ş and Uslu İ 2016 *Compos. Part B* **98** 260
- [12] Demirezen S, Altındal Ş and Uslu İ 2013 *Curr. Appl. Phys.* **13** 53
- [13] Vearey-Roberts A R and Evans D A 2005 *Appl. Phys. Lett.* **86** 072105
- [14] Chandar Shekar B, Veeravazhuthi V, Sakthivel S, Mangalaraj D and Narayandass S K 1999 *Thin Solid Films* **348** 122
- [15] Reddy M S P, Kang H S, Lee J H, Reddy V R and Jang J S 2014 *J. Appl. Polym. Sci.* <https://doi.org/10.1002/app.39773>
- [16] Yakuphanoglu F and Şenkal B F 2007 *J. Phys. Chem. C* **111** 1840
- [17] Özdemir A F, Akcan D E, Lapa H E, Yavuz A G and Duman S 2015 *Acta Phys. Polym. A* **128** B-450
- [18] Bilkan Ç, Zeyrek S, San S E and Altındal Ş 2015 *Mater. Sci. Semicond. Process.* **32** 137
- [19] Soylu M 2011 *Mater. Sci. Semicond. Process.* **14** 212
- [20] Özdemir A F, Aldemir D A, Kökce A and Altındal S 2009 *Synth. Met.* **159** 1427
- [21] Chatterjee B, Kulshrestha N and Gupta P N 2016 *Measurement* **82** 490
- [22] Hemalatha K S, Sriprakash G, Prasad M V N A, Damle R and Rukmani K 2015 *J. Appl. Phys.* **118** 154103
- [23] Nicollian E H and Brews J R 1982 *MOS (metal oxide semiconductor) physics and technology* (New York: Wiley)
- [24] Bilkan Ç, Azizian-Kalandaragh Y, Altındal Ş and Shokrani-Havigh R 2016 *Physica B* **500** 154
- [25] Şafak Asar Y, Asar T, Altındal Ş and Özçelik S 2015 *Philos. Mag.* **95** 2885
- [26] MacCallum J R and Vincent C A 1989 *Polymer electrolyte reviews* (London: Elsevier)
- [27] Sattar A A and Rahman S A 2003 *Phys. Stat. Sol. (a)* **200** 415
- [28] Dutta P, Biswas S and De S K 2002 *Mater. Res. Bull.* **37** 193
- [29] Çetinkaya H G, Alialy S and Altındal Ş 2016 *J. Mater. Sci. Mater. Electron.* **26** 3186
- [30] Afandiyeva I M, Bülbül M M, Altındal Ş and Bengi S 2012 *Microelectron. Eng.* **93** 50
- [31] Demirezen S 2013 *Appl. Phys. A* **112** 827
- [32] Jayalakshmi M and Balasubramanian K 2008 *Int. J. Electrochem. Sci.* **3** 1196
- [33] Khan N A, Mumtaz M and Khurram A A 2008 *J. Appl. Phys.* **104** 033916
- [34] Song X, Fu R and He H 2009 *Microelectron. Eng.* **86** 2217
- [35] Chaabane I, Hlel F and Guida K 2008 *J. Alloys Compd.* **461** 495
- [36] Demirezen S, Kaya A, Altındal Ş, Yerişkin S, Balbaş M and Uslu İ 2016 *Res. Phys.* **6** 180